CSM
Chemistry of Solid Materials
Vol. 2 No. 1 2014

Synthesis and characterization of amine functionalized mesoporous magnetite nanoparticles having environmental applications

M. Khabazipour[1], Sh. Shariati*[2]
[1]*MSc Student, Department of Chemistry, Islamic Azad University, Rasht Branch, Rasht, Iran.*
[2]*Associate Professor, Department of Chemistry, Islamic Azad University, Rasht Branch, Rasht, Iran.*

** Corresponding author's E-mail: Shariaty@iaurasht.ac.ir*

Article history:
(Received: 10 Jun 2014, Revised: 9 Aug 2014, Accepted: 16 Aug 2014)

ABSTRACT

In this study, amino functional groups were chemically bonded to the surface of newly synthesized KIT-6 mesoporous magnetite nanoparticles (MMNPs) by post-toluene reflux synthesis method. This method treats calcined mesoporous nanoparticles with the functional organosilanes. Physical and chemical structures of the synthesized mesoporous magnetite nanoparticles were characterized by scanning electron microscopy (SEM), powder X-ray diffraction (XRD), Fourier transform infrared spectroscopy (FT-IR) and nitrogen adsorption-desorption isotherms. Finally, the ability of the newly synthesized aminated mesoporous magnetite nanoparticles as a novel and recoverable sorbent with environmental applications was examined by studying the removal of dichromate ions from aqueous samples.

Keywords: KIT-6, Mesoporous magnetite nanoparticles, Amine functionalized

1. INTRODUCTION

Various methods for water refinement have been developed and used. Adsorption is one of these methods, which is a fast, inexpensive and widely applicable technique [1]. Mesoporous materials are very attractive for separation and adsorption processes due to their high specific surface area, large pore volume, regular structure, uniform pore size distribution and relatively high thermal stability [2]. Mesoporous silica materials like MCM-n, SBA-n and Kit are fairly new types of material that have pores in the mesoscopic range of 2–50 nm. The synthesis of magnetite nanoparticles coated with mesoporous silica leads to an improvement in the surface area and in the textural properties of the magnetite nanoparticles which in turn, provides more stable supports for various organic and inorganic species. Many efforts have been made to prepare metal-fill in mesoporous through post-synthesis grafting procedures or direct synthesis [3]. However, it is very difficult to introduce the metal ions into mesoporous directly due to the facile dissociation of metal-O-Si bonds under strong acidic hydrothermal conditions [4-7]. Most of the works have been focused on the post-synthesis method. But the post-synthesis method always forms metal oxides in the channels or external surface of the support, which would block the channels and not allow the reactants to access all the reaction sites in the porous matrix [8-10].

Here, we report a simple and effective procedure for successful preparation of mesoprous KIT-6 magnetite nanoparticles with high surface area. For the surface modification of KIT-6 coated magnetite with an NH_2 linker, aminopropyltriethoxysilane (APTES) was used as the surface modification agent. Surface modification or functionalization of mesoporous materials is a great technique for removal of some organic and inorganic contaminants [11]. In this context, aliphatic hydrocarbons [12], phenyl [13], amine [14], thiol and sulfonic functionalities have been mainly studied as surface modifiers. Among these useful functional groups, amine groups represent great potential for metal ion extraction [15], molecular gates [16], sensors, adsorption [17] and catalysts [18]. In the present research, the synthesis of new mesoporous magnetite nanoparticles with a high density of amino groups is studied. This strategy involves Fe_3O_4 nanoparticle as the magnetic core coated by SiO_2 and after that KIT-6 mesoporous silica as a thin layer to form a core/shell structure that is functionalized by amine via post synthesis method. In this method, organic functional groups are covalently attached to the silanol groups (Si–OH) of the pore surface by the reaction of the organosilane under reflux condition in toluene solvent. To the best of our knowledge, this is the first report on the synthesis and application of this newly synthesized MMNPs.

2. EXPERIMENTAL

2.1. Material

Ferric chloride hexahydrate ($FeCl_3$-$6H_2O$), ferrous chloride tetrahydrate ($FeCl_2.4H_2O$), sodium hydroxide, tetraethylorthosilicat (TEOS), 3-aminopropyltriethoxysilane (H_2N-$CH_2CH_2CH_2Si(OC_2H_5)_3$, APTES) as organosilane, potassium dichromate, *n*-butanol, *p*-toluenesulfonic acid, absolute ethanol and hydrochloric acid (37 wt %) were purchased with high purity from Merck (Darmstadt, Germany). Pluronic P123 (EO_{20}–PO_{70}–EO_{20}, MW=5800) as a non-ionic surfactant was prepared from Aldrich (Milwaukee, WI, USA). All stock and working solutions were prepared using doubly distilled water.

2.2. Instrumentation

The crystal phases and crystallinity of synthesized MMNPs were analyzed on X-PRTPRO (PANalitical, Netherlands) X-ray diffraction (XRD) instrument using Cu K_α radiation source with 2θ range of 0.5-70^o. To investigate the chemical structure of synthesized MMNPs, Shimadzu Fourier transform infrared spectrophotometer (FT-IR-470, Japan) in the wave number range of 400-4000 cm^{-1} was used. Nitrogen adsorption-desorption experiments for determination of surface area and pore size of the nanoparticles were carried out at 77 K (Bel, Japan). The size and morphology of the modified nanoparticles were observed under a Philips XL 30 scanning electron microscope (SEM, Netherlands). For absorption measurements a Shimadzu UV-Vis spectrophotometer (3100 pc series, Japan) was used. pH of solutions were measured by using a Crison pH meter (Basic 20, Spanish). For magnetic separation a strong super magnet with 1.4 T magnetic field (1 × 3 × 5 cm) were applied.

2.3. Synthesis of silica coated magnetite nanoparticles (Fe_3O_4@SiO_2 MNPs)

Fe_3O_4 MNPs were chemically synthesized with addition of an aquoues solution of ferous and ferric ions (in a 1:2 molar ratio) to amonia solution with little modification in the methodology already described in the literature [19]. Briefly, 10.4 g of $FeCl_3.6H_2O$, 4.0 g of $FeCl_2.4H_2O$ and 1.7 ml of HCl (12 mol L^{-1}) were dissolved in 50 ml of deionized water in order to prepare stock solution of ferrous and ferric chloride. This solution was degassed with purging nitrogen gas (99%) for 20 min. Simultaneously, 250 ml of 1.5 mol L^{-1} ammonia solution was degassed (for 15 min) and heated to 80 ^{o}C in a reactor. Then, the stock solution was slowly added to the ammonia solution using a dropping funnel during 60 min under nitrogen gas atmosphere and vigorous stirring (1000 rpm) by magnetic stirrer. During the whole process, the solution temperature was maintained at 80 ^{o}C and nitrogen gas was purged to remove the dissolved oxygen. After completion of the reaction, the obtained Fe_3O_4 MNPs were separated from the reaction medium by a magnet (1.4 Tesla), and then washed with 500 ml doubly distilled water four times. Finally, the obtained Fe_3O_4 MNPs were dried for 120 min at 90 ^{o}C. Due to instability of Fe_3O_4 MNPs under acidic condition for KIT-6 mesoporous synthesis, a silica layer was coted on the surface of synthesized particles. For synthesis of $Fe_3O_4@SiO_2$ MNPs, 1.0 g of the synthesized MNPs were homogeneously dispersed in 500 ml of ethanol containing ammonia (25 ml, 25 wt %), under stirring at 80^{o}C followed by dropwise addition of ethanolic solution of TEOS (10.8 %v/v). After stirring at 80 ^{o}C for 2 h, the $Fe_3O_4@SiO_2$ nanoparticles were obtained and washed several times with a mixture of water-ethanol (1:1). Then, the synthesized nanopartices dried at 100°C for 5 h.

2.4. Synthesis of KIT-6 mesoporous magnetite nanoparticles (Fe_3O_4@ SiO_2@KIT-6 MMNPs)

The KIT-6 mesoporous silica with cubic *Ia3d* symmetry as shell on the magnetite core was synthesized according to the method described in the literature [20]. Typically, 1.25 g of Pluronic P123 was dissolved in 45 ml of distilled water. Then, 1 g of $Fe_3O_4@SiO_2$ and 2.4 ml of HCl solution (37 wt %) were added to the solution under vigorous stirring. After complete mixing, 1.3 g of *n*-butanol (99.4 wt %) was added. Following further stirring for 1 h, 2.7 g of TEOS (as silica source) was added immediately. Subsequently, the mixture was left stirring at 35°C for 24 h and transferred into an autoclave, which was sealed and maintained at 100°C for another 24 h under static conditions. The resulting solid product was filtered and dried at 100°C overnight. After that, the filtrate was stirred for 1 h in a mixture of 300 ml EtOH containing 20 ml concentrated HCl (37 wt %). After ethanol/HCl washing, the final nanoparticles were filtered, dried at 90 °C and finally calcined at 550 °C for 6 h in air.

2.5. Synthesis of amine functionalized KIT-6 mesoporous magnetite nanoparticles ($Fe_3O_4@SiO_2$@KIT-6-NH_2 MM NPs)

Synthesis of amine functionalized MMNPs was carried out by the post-synthesis grafting method [21]. A post-synthesis grafting method is based on the silylation of surface silanol groups with organoalkoxysilanes. A detailed experimental description for synthesis of $Fe_3O_4@SiO_2$@KIT-6-NH_2 MMNPs is as follows: 0.5 g of synthesized KIT-6 mesoporous magnetite was dispersed in 75 ml of toluene by stirring for 0.5 h at 50 °C. After that, 3.5 mg of *p*-toluenesulfonic acid and 1.0 mmol of organosilane (APTES) were added to the mixture. The mixture was heated up to 120 °C and stirred for 4 h. After refluxing for 4 h, the solid product was filtered and washed with absolute ethanol several times and was dried at 100 °C for 12 h [21]. Figure 1 (a-d) shows the colour of synthesized nanoparticles during different steps.

Fig.1. Samples synthesized: (a) Fe_3O_4 (b) Fe_3O_4@SiO_2 (c) Fe_3O_4@SiO_2@KIT-6 (d) Fe_3O_4@SiO_2@KIT-6-NH_2

3. RESULTS AND DISCUSSION

3.1. Characterization of the synthesized MMNPs

IR spectra of Fe_3O_4@SiO_2@KIT-6-NH_2 MMNPs is shown in Figure 2. The bands at ~557 and 439 cm^{-1} are attributed to the Fe-O vibration of Fe_3O_4 in tetrahedral and octahedral sites, respectively. Also, the peak at ~1049 cm^{-1} is attributed to asymmetric stretching vibrations of Si-O-Si and stretching vibration of the N-H functionalities was observed at 3429 cm^{-1}.

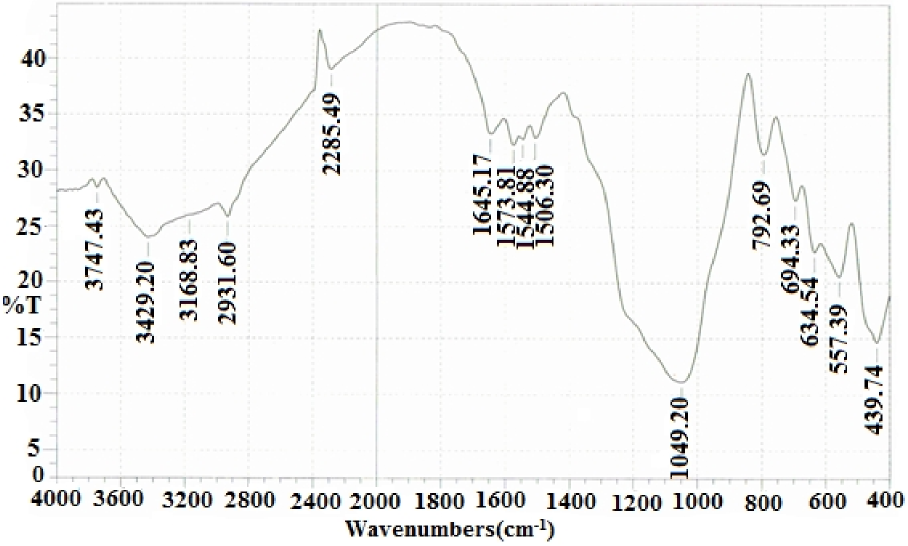

Fig. 2. FT-IR spectra of Fe_3O_4@SiO_2@KIT-6-NH_2 MMNPs

Figure 3 shows the XRD patterns of KIT-6 (A) and $Fe_3O_4@SiO_2@KIT\text{-}6\text{-}NH_2$ in low(B) and wide (C) angels. Three peaks with 2θ at 1, 1.6 and 1.83, indicating well resolved (211), (220) and (332) peaks which are typical for cubic order materials with *la3d* space group. Other peaks with 2θ at 26.05, 30.315, 35.66, 43.35, 53.8, 57.3, 62.96 and 71.51 correspond to Fe_3O_4. As shown in Figure, the intensities of XRD patterns decrease and d spacing was shifted to small angle with the increase of mesopores coating on the iron oxide core. It seems that absence of the prominent peaks revealed the mesostructure would collapse with iron oxid core, compared to that of the mesoporous KIT-6.

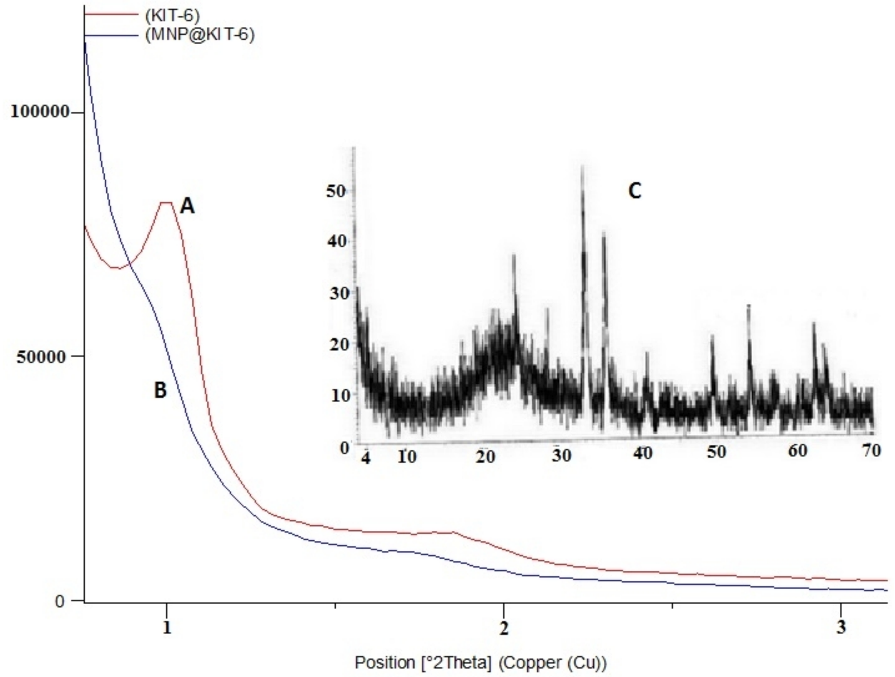

Fig. 3. (A) X-ray diffraction pattern of KIT-6, (B) $Fe_3O_4@SiO_2@KIT\text{-}6\text{-}NH_2$ in small angle and (C) $Fe_3O_4@KIT\text{-}6\text{-}NH_2$ in wide angle.

Nitrogen adsorption–desorption isotherm of the MMNPs show a characteristic type IV curve (Figure 4A) with a distinct hysteresis loop in the p/p_0 range of 0.6–0.9, indicating the presence of a narrow distribution of mesoporous pore size. The type IV isotherm (IUPAC classification) is typical for mesoporous systems. The typical BJH (Barrett– Joyner–Halenda) pore size distributions (Figure 4B) indicates narrow pore size distributions for samples. A comparison between the BET and XRD results of the synthesized sorbent with other reported mesoporous samples are summarized in Table 1. The results clearly indicate that the core/shell structure of MMNPs has high surface areas, large and uniform pores. Therefore, it could be deduced that the pores of the silica mesoporous shell were remained after loading on the surface of iron oxide nanoparticles.

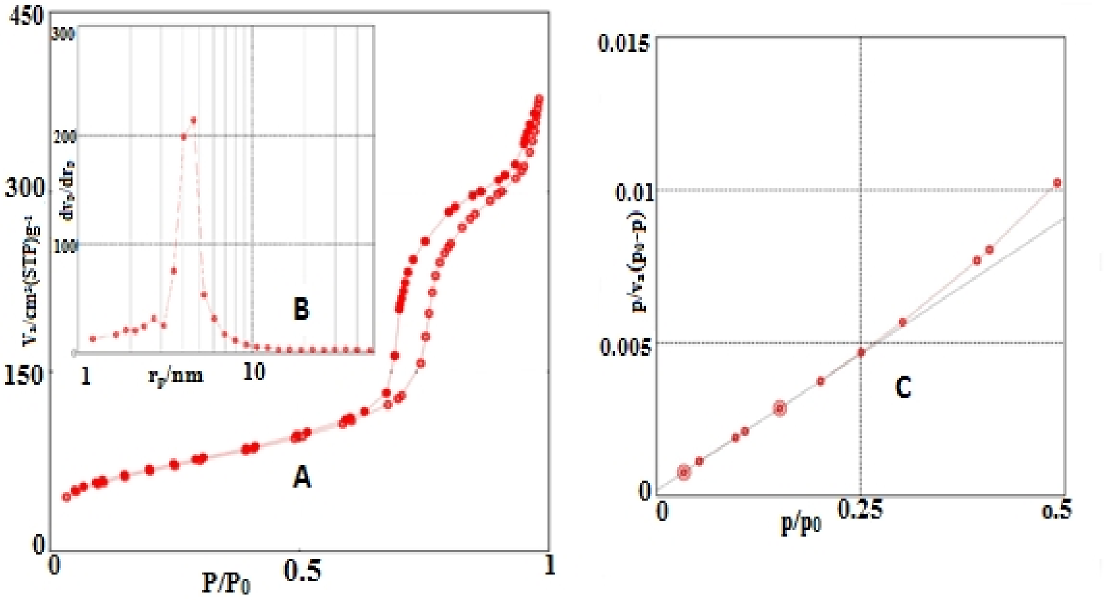

Fig. 4. (A) Nitrogen adsorption-desorption isotherms measured at 77K; (B) pore size distribution curves (inset) of core–shell structured synthesized and BET (C) of Fe_3O_4@SiO_2@ KIT-6.

Table 1: A comparison between the BET and XRD results of the synthesized nanoparticles with other reported mesoporous samples.

	Fe_3O_4@SiO_2@ KIT-6	KIT-6- α-Fe_2O_3 [22]	SPIO@mSiO_2 [23]	ASP–Fe_3O_4@MCFS [24]
S_{BET} [m^2g^{-1}]	241.68	148	46	140
a_p[m^2g^{-1}]	224.84	-	-	-
V_{total}[cm^2g^{-1}]	0.583	-	-	-
V_p[cm^2g^{-1}]	0.566	0.47	0.0813	0.36
$d_{0(BJH)}$[nm]	9.25	2.7	7.03	10.3
W (nm)	2.84	-	-	-
d_{100}/d_{211}	99.20	-	-	-

BET surface area calculated in the range of relative pressure (p/p0) = 0 - 0.5
d_o = mean pore dimeter (BJH)
V_{tot} = total pore volumes measured at (p/p_0) =0.98
V_p= mean volume of the pores
a_p= surface of pores
d = d-spacing
a = unitcell parameter
w = wall thickness

Figure 5 shows the SEM image of the synthesized $Fe_3O_4@SiO_2@KIT$-6 nanoparticles. As seen in image, the morphologies are very uniform and spherical nanoparticles with diameters about 17 nm were synthesized.

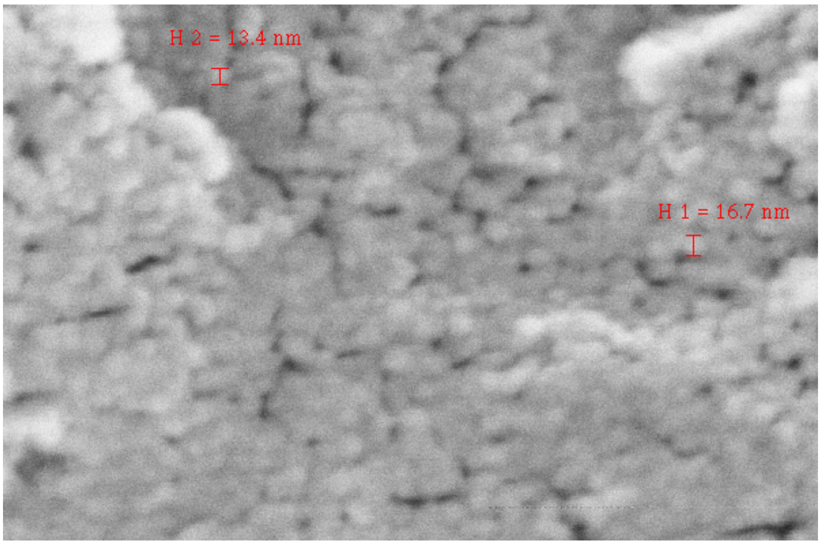

Fig. 5. SEM micrograph of $Fe_3O_4@SiO_2@KIT$-6 MMNPs

3.2. Application of synthesized amine functionalized MMNPs

The newly synthesized amine functionalized MMNPs were good sorbents for removal of the anionic species from aqueous solutions. At acidic pHs, amino groups have positive charges and can be linked to anionic species via electrostatic interaction. The ability of the aminated mesoporous magnetite was examined for the removal of Cr(VI) in hydrogenchromate ($HCrO_4^-$) form as model anionic compound from aqueous solutions. A solution of 150 mg L^{-1} Cr(VI) was prepared by dissolving a known quantity of potassium dichromate ($K_2Cr_2O_7$) in double-distilled water. The equilibrium studies were systematically carried out in a batch process, covering various process parameters. Different species of Cr(VI) ($Cr_2O_7^{2-}$, $HCrO_4^-$, $Cr_3O_{10}^{2-}$, $Cr_4O_{13}^{2-}$) coexist at acidic pH condition. At pH 2–3 the predominant Cr(VI) species is $HCrO_4^-$, which is favorable adsorbed since it has a low adsorption free energy.

$$2CrO_4^{2-} + 2H^+ \rightleftharpoons 2HCrO_4^- \rightleftharpoons H_2O + Cr_2O_7^{2-}$$

The maximum Cr(VI) adsorption capacity, calculated via absorption spectrophotometry measurements, was obtained as 185.18 mg g^{-1} at the optimal conditions (Sample volume: 75 ml, pH=2, contact time: 15 min, MMNPs dose: 1 g L^{-1}). Cr(VI) ions were desorbed with alkali solutions. The obtained magnetite was reused for the Cr(VI) adsorption for 4 cycles with Cr(VI) removal efficiency higher than 90%. A comparison between the newly synthesized MMNPs with the other reported sorbents for removal of Cr(VI) pollutant was summarized in Table 2. According to results, very good sorption capacity was achieved in a relatively shorter time that confirm the potential of these nanoparticles for Cr(VI) removal.

Table 2. A comparision between the apllicability of proposed sorbent with other reported sorbents in Cr(VI) removal.

Adsorbents	pH	Contact Time (h)	Dose of Adsorbent (g L-1)	Adsorption Capacity (mg g-1)	References
NH_2 functionalized KIT-6 mesoporous magnetite	2	0.25	1	185.2	This Work
Activated carbon-based iron containing adsorbents	2	48	0.6	68.49	[25]
Hevea Brasilinesis sawdust activated carbon	2	5	0.1	44.05	[26]
Modified, cationic surfactant spent mushroom	3.39	1.15	5	43.86	[27]
Chemically activated Neem Sawdust	4	3	6	24.63	[28]
Peanut shell	4	6	0.4	4.32	[29]
Oxidized activated carbon from peanut shell	2	24	0.1	14.54	[30]
Poly- (methyl acrylate) fuctionalized guar gum	1	24	4	29.67	[31]
Mesopore of Activated Carbon	3	48	2	53.8	[32]
Immobilized mycelia in carboxy methyl-cellulose (CMC) of Lentinus sajor-caju	2	2	25	32.2	[33]

4. CONCLUSION

In this study, well-ordered amine functionalized KIT-6 mesoporous magnetite nanoparticles were chemically synthesized. The resultant materials showed good crystallographic order and large uniform pore size. Surface functionalization of synthesized MMNPs with amino groups produces good properties to sorbent for magnetically removal of anionic species as well as for solid phase extraction of trace amounts of analytes and induces optimum interaction between sorbent and adsorbate. The proposed regenarable nanoparticles are synthesized easily and separated via magnet. Due to their very high surface areas, high sorption capacity can be achieved in short exposure times. These nanoparticles are useful for the design of an economically treatment process for removal of anionic pollutants.

Acknowledgement

Financial support by Rasht Branch, Islamic Azad University Grant No. 4..5830 is gratefully acknowledged.

REFERENCES

[1] M. Anbia, M. B. Ghasemian, Sh. Shariati, *Anal. Methods.*, 4, 4220 (**2012**).

[2] J. S. Beck, J. C. Vartuli, W. J. Roth, M. E. Leonowicz, C. T. Kresge, K. D. Schmitt, C. T. Chu, D. H. Olson, E. W. Sheppard, S. B. McCullen, J. B. Higgins, J. L. Schlenker, *J. Am. Chem. Soc.,* 114, 10834 (**1992**).

[3] S.W. Chen, C. W. Ma, M. M. Qin, H. F. Yang, H. Y. Xie, J. Guan, *React. Kinet. Mech. Cat.* 106, 245 (**2012**).

[4] A. Cedeon, A. Lassoued, J. L. Bonardet, J. Fraissard, *Micro. Meso. Mater*., 801, 44-45, (**2001)**.

[5] W. H. Zhang, J. Lu, B. Han, M. Li, J. Xiu, P. Ying, C. Li, *Chem. Mater.,* 14, 3413 (**2002)**.

[6] B. L. Newalkar, J. Olanrewaju, S. Komarneni, *Chem. Mater.,* 13, 552 (**2001)**.

[7] Wu, S.; Han, Y.; Zou, Y. C.; Song, J. W.; Zhao, L.; Di, Y.; Liu, S. Z.; Xiao, F. S. *Chem. Mater.* 16, 486 (**2004)**.

[8] M. S. Morey, S. O'Brien, S. Sch Warz, G. D. Stucky, *Chem. Mater.,* 12, 898 (**2000)**.

[9] M. J. Cheng, Z. Wang, K. Sakurai, F. Kumata, T. Saito, T. Komatsu, T. Yashima, *Chem. Lett.,* 2, 131(**1999)**.

[10] S. Sumiya, Y. Oumi, T. Uozumi, T. Sano, *J. Mater. Chem.,* 11, 1111 (**2001)**.

[11] A. Vinu, K.Z. Hossian, P. Srinivasu, M. Miyahara, S. Anandan, N. Gokulakrishnan, T. Mori, K. Ariga ,V.V. Balasubramanian., *J. Mater. Chem.,* 17, 1819 (**2007**).

[12] L. Mercier, T. J. Pinnavaia, *Chem. Mater.,* 12, 188 (**2000**).

[13] M.C. Burleigh, M. A. Markowitz, M. S. Spector, B. P. Gaber, *J. Phys. Chem.* 105, 9935 (**2001**).

[14] Q. Wei, Z. R. Nie, Y. L. Hao, L. Liu, Z. X. Chen, J. X. Zou, *J. Sol. Gel. Sci. Tech.,* 39, 103 (**2006**).

[15] J. Aguado, J. M. Arsuaga, A. Arencibia, M. Lindo, V. Gascon, *J. Hazard. Mater.* 163, 213 (**2009**).

[16] R. Casasús, M.D. Marcos, R. Martínez-Máñez, J.V. Ros-Lis, J. Soto, L.A. Villaescusa, P. Amorós, D. Beltrán, C. Guillem, J. Latorre, *J. Am. Chem. Soc.,* 126, 8612 (**2004**).

[17] S. Saeung, V. Boonamnuayvitaya, *J. Environ. Sci.,* 20, 379 (**2008**).

[18] S. L. Hruby, B. H. Shanks, *J. Catal.,* 263, 181 (**2009**).

[19] N. Saadatjoo, M. Golshekan, Sh. Shariati, H. Kefayati, P. Azizi, *J. Mol. Catal. A-Chem* 377, 173 **(2013).**

[20] F. Kleitz, S. H. Choi, R. Ryoo, Chem. Commun., 17, 2136 (**2003**).

[21] N. Garcia, E. Benito, J. Guzman, P. Tiemblo, V. Morales, R.A. Garcia, *Micropor. Mesopor. Mater.,* 106, 129 (**2007**).

[22] J. K. Shon, S. S. Kong, S. S. Kim, M. S. Kang , J. M. Kim, *Funct. Mater. Lett,* 1, 151 (**2008**).

[23] J. M. Rosenholm, J. Zhang, W. Sun, H. Gu, *Micro. Meso. Mater.,* 14, 5 14 (**2011**).

[24] Sh. Huang, Ch. Li, Z. Cheng, Y. Fan, P. Yang, C. Zhang, K. Yang, J. Lin, *J. Colloid interface Sci.,* 376, 312 (**2012**).

[25] W. Liu, J. Zhang, C. Zhang, L. Re, *Chem. Eng. J.,* 189, 295 (**2012**).

[26] T. Karthikeyan, S. Rajgopal, L. R. Miranda, *J. Hazard. Mater.,* 124, 192 (**2005**).

[27] X. Jing, Y. Cao, X. Zhang, D. Wang, X. Wu, H. Xu., *Desalination,* 269, 120 (**2011**).

[28] A. Saran, H. Kumar, P. Shrivastava, *Middle. East. J. Sci. Res.,* 17, 936 (**2013**).

[29] M. Liyas, A. Ahmad, M. Saeed, *J. Chem. Soc. Pak.,* 35, 760 (**2013**).

[30] Z. A. Alothman, R. Ali, M. Naushad, *J. Chem. Eng.,* 184, 238 (**2012**).

[31] V. Singh, P. Kumari, S. Pandey, T. Narayan, *Bioresour. Technol.* 100, 1977 (**2009**).

[32] L. Mao, F. Minxia, Sh. Tong, *Environ. Division.,* 749, 465 (**2012**).

[33] M. Y. Arıca, G. Bayramoglu, *Colloid. Surf. A.,* 253, 203 (**2005**).